Front. Optoelectron. China 2009, 2(1): 21–27
DOI 10.1007/s12200-009-0009-9

RESEARCH ARTICLE

All-optical clock extraction for CSRZ modulation data

Zhixin CHEN (✉), Xin JIN, Huaihu CAO, Jian WANG

School of Information, Central University of Finance and Economics, Beijing 100081, China

Abstract This paper demonstrates a theoretical investigation on clock extraction from carrier-suppressed return-to-zero (CSRZ) modulation format data at 40 Gbit/s by using a semiconductor optical amplifier (SOA)-based ring laser. A completely numerical analysis about the clock characteristics at 40 Gbit/s is done, which is an effective guide for the experiment and necessary to optimize system performance. The crucial parameters, including the pulse width, energy of the CSRZ data signals and influence of SOA bias current, are analyzed because they determine the quality of the recovered clock pulses. Meanwhile, simulation results show that high-quality clock extraction from 2^7–1 pseudo-random binary sequence (PRBS) CSRZ data at 40 Gbit/s can be achieved by using higher power assisting continuous-wave (CW) light into a SOA-based ring laser.

Keywords all-optical signal processing, all-optical clock extraction, semiconductor optical amplifier (SOA), cross gain modulation (XGM), carrier-suppressed return-to-zero (CSRZ) modulation

1 Introduction

All-optical clock extraction is one of the key technologies for realizing high-speed optical networks that require synchronous operations such as re-amplification, re-shaping and re-timing (3R). Several schemes for all-optical clock extraction have been reported. A scheme based on self-pulsating laser diodes, which is easy to integrate but requires complicated technologies, has been demonstrated at 40 Gbit/s [1]. Clock extraction configuration based on mode-locked semiconductor lasers has been realized at 160 Gbit/s, but the weakness of this structure is unstable [2]. Optoelectronic phase-locked loop (OPLL) can be also used for all-optical clock extraction, but this scheme requires high-injected power and the operation speed is limited because of electronic barriers [3]. Injection mode-locked fiber laser based on a semiconductor optical amplifier (SOA) is one of the promising methods for all-optical clock extraction, as it may provide high quality clock pulses and can work at a high bit rate. The advantage of using SOA as a nonlinear switching medium also holds fast recovery time and can be integrated with other semiconductor components [4].

In recent years, novel modulation formats have been intensively studied in high-speed transmission systems. The optical carrier-suppressed return-to-zero (CSRZ) modulation format is considered one of the promising transmission signal formats in dense wavelength division multiplexing (DWDM) systems and is currently widely used in long-haul transmission systems due to its high fiber nonlinearity tolerance [5–7]. However, previous clock extraction schemes are usually applied to common modulation formats, such as return-to-zero (RZ) and non-return-to-zero (NRZ), and there is no research report on clock extraction from CSRZ data. Therefore, clock extraction for CSRZ data is imperative. To the authors' best knowledge, a detail theoretical analysis on clock extraction at 40 Gbit/s based on SOA-based ring laser from CSRZ modulation format data has not yet been reported.

In this paper, all-optical clock extraction using an SOA-based ring laser from CSRZ modulation format data is investigated for the first time. A numerical model is given and the simulation result shows this scheme is still an effective technology for implementing clock extraction in case of a high bit rate (about 40 Gbit/s) and novel modulation format. Some critical parameters that have great influence on the performance of extracted clocks are investigated numerically, including the pulse width, energy of CSRZ data signals and bias current of SOA.

2 Principle and numerical model

Figure 1 shows the schematic diagram of clock extraction based on an SOA-based ring laser. The CSRZ data signal is injected into the cavity through coupler C_1 and the extracted clock pulses export from coupler C_2. SOA is the key element for clock extraction, which provides gain

Received August 8, 2008; accepted October 17, 2008

E-mail: czx.bupt@gmail.com

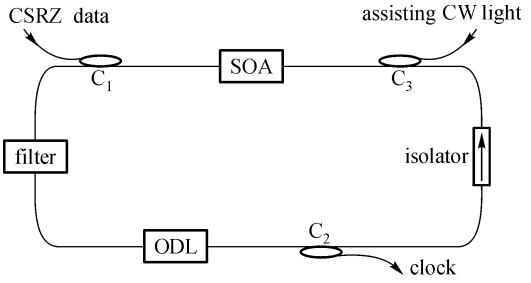

Fig. 1 Clock extraction configuration based on an SOA-based ring laser

and gain modulation in this scheme. Because of the cross gain modulation (XGM) effect in SOA, the gain in the ring cavity is periodically modulated by the injected CSRZ data signal, which causes the generation of mode-locking pulses (i.e., the recovered clock pulses) with repetition rate equaling the rate of the CSRZ data signal [8,9]. A tunable optical filter is used for selecting desirable wavelength clock pulses, an isolator ensures unidirectional oscillation of the clock pulses and blocks of CSRZ data, and an optical delay line (ODL) is used to precisely adjust the cavity length to obtain clock pulses at the expected repetition rate. The assisting continuous-wave (CW) light is injected into the cavity through coupler C_3, which is mainly used to eliminate pattern effects caused by the slow gain-extraction of SOA [10,11].

A numerical model based on a self-reproducing pulse profile model has been given by Ref. [8], in which the clock pulse in the cavity can reproduce itself after each complete transit through the SOA, filter and other components when laser is at a steady state. In this model, amplified spontaneous emission (ASE) noise of SOA is neglected due to the high power of both CSRZ data and clock signals that deeply saturate the SOA. As the pulse-width of CSRZ data is less than 10 ps, the nonlinear gain compression in SOA is mainly contributed by the intra-band effects of SOA such as carrier heating (CH) and spectral hole burning (SHB). Therefore, the carrier density rate equation, optical power and nonlinear phase shift in each section of the SOA can be expressed as [10]

$$\frac{\partial N_j(z,t)}{\partial t} = \frac{I}{qV} - (c_1 N_j + c_2 N_j^2 + c_3 N_j^3) - \sum_{k=1,2,3} \frac{\Gamma g_{k,j} P_{k,j}}{h\nu_k A(1+\varepsilon P_j)}, \quad (1)$$

$$\frac{\partial P_{k,j}(z,t)}{\partial z} = \left(\frac{\Gamma g_{k,j}}{1+\varepsilon P_j} - \alpha_{\text{int}}\right) P_{k,j}(z,t), \quad (2)$$

$$\frac{\partial \phi_{k,j}(z,t)}{\partial z} = -\frac{\alpha_k}{2}\frac{\Gamma g_{k,j}}{1+\varepsilon P_j}, \quad (3)$$

where subscript $j = 1,2,...,n$ stands for section number, and $k = 1,2,3$ denotes the CSRZ data, clock and assisting CW light, respectively. $N_j(z,t)$ is the carrier density in section j, I is the injected current, q is electron charge, V is the volume of active region. c_1 is the nonradiative recombination coefficient caused by defects and traps, c_2 is the bimolecular recombination coefficient and c_3 is the Auger recombination coefficient. Γ is the mode confinement factor, $g_{k,j}$ is the material gain for beam k in section j, h is the Planck constant, ν_k is the optical frequency of beam k, A is the cross-sectional area of the active region, ε is the nonlinear gain compression effects produced by CH and SHB effects, P_j is the sum power in section j, and $P_{k,j}(z,t)$ and $\phi_{k,j}(z,t)$ are the power and phase shift of beam k in section j, respectively. α_{int} is the internal loss of SOA, and α_k is linewidth enhancement factor, which can be estimated by

$$\alpha_k = -\frac{4\pi}{\lambda_k}\frac{\mathrm{d}n/\mathrm{d}N}{a}, \quad (4)$$

where λ_k is the wavelength of beam k, $\mathrm{d}n/\mathrm{d}N$ is differential refractive index, and a is the empirically determined constant. A cubic formula with empirically determined constants is used to model the asymmetric gain spectrum of SOA [11]:

$$g = a(N-N_{\text{t}}) - \gamma_1(\lambda-\lambda_{\text{p}})^2 + \gamma_2(\lambda-\lambda_{\text{p}})^3, \quad (5)$$

$$\lambda_{\text{p}} = \lambda_{\text{t}} - \kappa_0(N-N_{\text{t}}), \quad (6)$$

where γ_1 and γ_2 are empirically determined constants, with γ_1 determined by gain bandwidth and γ_2 accounting for the asymmetry of the curve; λ is the wavelength of the light in consideration; λ_{p} is the gain peak wavelength for carrier density; N_{t} is the carrier density at transparency; λ_{t} is the gain peak wavelength at transparency; and κ_0 is the gain peak shift coefficient.

When there is no optical input into the SOA, a steady state can be established under certain current levels, which can be characterized by carrier density N_0 and carrier lifetime τ. When a CW light is injected into the SOA, a steady state can be also built in the active region of SOA, but the carrier density and carrier lifetime change. The effective carrier lifetime τ_{eff} can be obtained by the following expression [10]:

$$\tau_{\text{eff}} = \frac{\tau}{1+P_{\text{a}}/P_{\text{s}}}, \quad (7)$$

where $P_{\text{s}} = \dfrac{h\nu A}{\Gamma a \tau}$ is the saturation power of SOA, ν is the optical frequency of data signal, and P_{a} is average power in the SOA active region:

$$P_{\text{a}} = \frac{1}{L}\int_0^L P_{\text{CW}}(z)\mathrm{d}z, \quad (8)$$

where L is the length of SOA and $P_{\text{CW}}(z)$ is the injection

power of assisting CW light in the SOA active region. Equation (1) is a steady state equation when only CW light exists, so $P_{CW}(z)$ can be solved using Eq. (1) and τ_{eff} can be obtained from Eq. (7). Equation (7) indicates that the carrier lifetime will decrease dramatically when an assisting CW light is injected into SOA.

The transmission function of the filter is expressed as a Gaussian function:

$$T(\omega) = \sqrt{1-\alpha_f}\exp\left[-(\omega-\omega_0)^2/B_f^2\right], \tag{9}$$

where α_f is the loss of filter in the center frequency , ω is the angle frequency of optical signals, ω_0 is the central angle frequency of filter, and B_f is related to the full width at half maximum (FWHM) ν_{FWHM} by

$$B_f = 2\pi\nu_{FWHM}/(2\sqrt{\ln 2}). \tag{10}$$

Equations (1)–(10) are the models used in simulation.

3 Simulation results and performance analysis

The bias current of SOA is set to 90 mA, and the peak gain wavelength of SOA is 746 nm. In simulation, it is assumed that the filter has a Gaussian profile with a bandwidth of 2.5 nm. Other physical parameters of the SOA used in simulation are taken from Refs. [10–12]. The 40 Gbit/s 2^7–1 pseudo-random binary sequence (PRBS) data with CSRZ modulation format is injected into ring cavity as well as an assisting CW light with the power of 25 dBm. For evaluating the amplitude fluctuation of the extracted clock pulses, the relative standard deviation R_s is defined as [13]

$$R_s = \frac{S}{M}\times 100\%, \tag{11}$$

where M and S are the mean amplitude and standard amplitude deviation of the clock pulses, respectively. The timing jitter is characterized by standard deviation of the time. Therefore, both amplitude fluctuation and timing jitter of the extracted clock pulses can be obtained by using Eq. (11) for every time in simulation as follows:

A typical result of clock extraction from 40 Gbit/s CSRZ data using an SOA-based ring laser is shown in Fig. 2. In the simulation, it is assumed that the pulsewidth of the input CSRZ data is 6 ps FWHM and the average injecting power is 5.44 dBm. Figures 2(a) and 2(b) show the sample waveform and optical spectrum of the injected 40 Gbit/s CSRZ data. Figures 2(c) and 2(d) show the waveform and optical spectrum of the extracted clock pulses without an assisting CW light. As can be seen, the waveform and optical spectrum have worse performances. The amplitude fluctuation is 41% and the timing jitter is about 4 ps by using Eq. (11), which means the pattern effect of the clock pluses is too significant to apply in 3R. To reduce the pattern effect, the assisting CW light is injected into the SOA-based ring laser. Figures 2(e) and 2(f) show the waveform and optical spectrum of the extracted clock pulses when the 25 dBm assisting CW light is injected into SOA. The amplitude fluctuation of clock pulses is estimated to be about 17% and the timing jitter is about 0.5 ps by using Eq. (11), which means there is still a slight pattern effect but weakened significantly due to the injection of the assisting CW light. The results above show that this method is an effective technology for all-optical clock extraction from CSRZ modulation format data using the SOA-based ring laser.

The dependence of pattern effect on the injection power of the assisting CW light is analyzed. Figure 3 shows τ_{eff} of SOA as a function of the input power of the assisting CW light. With increasing injection power of the assisting CW light, τ_{eff} of SOA is gradually decreasing. When there is no light input, τ_{eff} of SOA is usually several hundred ps governed by the spontaneous emission. However, when the assisting CW light in gain region or at the transparency wavelength is injected, new carriers are generated and the gain recovery is enhanced due to absorption. This results in the pattern effect being reduced rapidly. Meanwhile, the carrier lifetime at the wavelength of the assisting CW light in the gain region can be reduced more effectively than that at transparency wavelength. When power of the assist light increases to about 30 dBm, SOA will be deeply saturated, and gain of the assisting CW light at different wavelengths tends to be the same value determined only by the material absorption coefficient. Recovery time for each wavelength tends to obtain the corresponding steady value [11].

Meanwhile, the dependence of pattern effect on wavelength of the assisting CW light is analyzed. Figure 4 shows τ_{eff} of SOA for different wavelengths of the assisting CW light. In terms of the short wavelength of SOA, the longer the wavelength, the smaller the pattern effect. In the long wavelength range, when the wavelength becomes longer, the pattern effect will correspondingly increase. Meanwhile, the peak wavelength is about 1550 nm. Thus, the minimum pattern effect occurs near the peak wavelength of gain curve of SOA, where the carrier lifetime recovery time is shortest. This can be simply explained as follows: for the assisting CW light near the gain peak of SOA, average optical power in the SOA active region is maximized and τ_{eff} is minimized. Thus, the lowest pattern effect will appear near the peak wavelength of SOA [11].

Figure 5 shows the dependency of the performance (clock pulsewidth, amplitude fluctuation and timing jitter) of the recovered clock pulses with the pulsewidth of injected CSRZ data. It can be seen from Fig. 5(a) that the pulsewidth of the recovered clock pulse becomes narrower with a decrease of the injected CSRZ data pulsewidth. This happens as shorter injected CSRZ data pulses pass faster through SOA without enough time bringing it to the saturation level required for the formation of the mode-

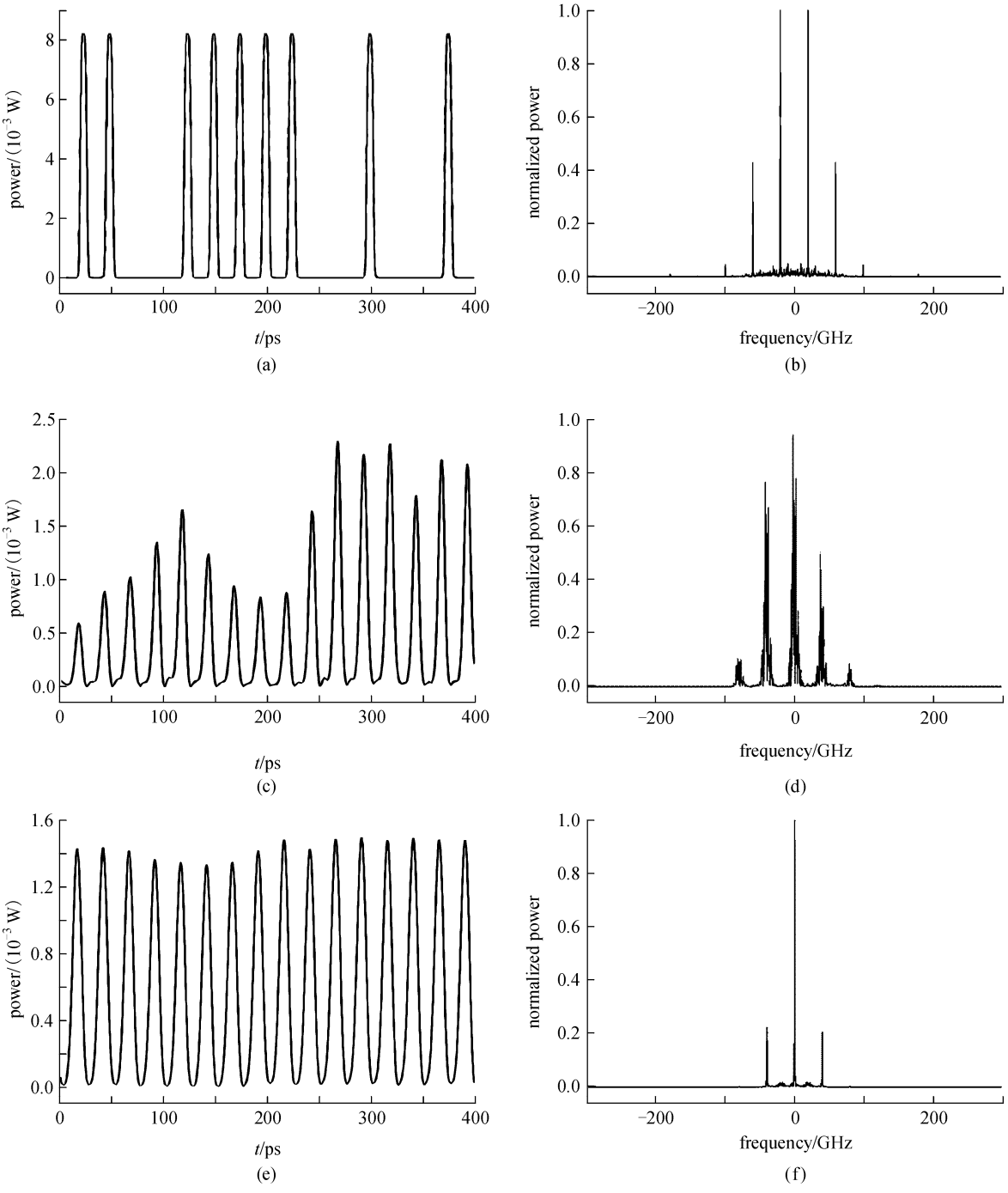

Fig. 2 Waveform (a) and optical spectrum (b) of injected CSRZ data streams at 40 Gbit/s; waveform (c) and optical spectrum (d) of recovered 40 GHz clock pulses without assisting CW light; waveform (e) and optical spectrum (f) of recovered 40 GHz clock pulses with assisting CW light

locked clock pulses, so that more energy is necessary. As a result, increasing the extracted clock's energy leads to a reduction of the clock pulsewidth. However, it can be indicated that the sensitivity of the output mode-locked clock pulsewidth on the injected CSRZ data pulsewidth is relatively weak. Figure 5(b) depicts the amplitude fluctuation and timing jitter as a function of the pulsewidth of injected CSRZ data. It is found that by increasing pulsewidth of the injected CSRZ data, the recovered clock signal amplitude fluctuation and timing jitter accordingly increase, which slightly weaken the quality of recovered clock pulses. However, for CSRZ data pulsewidth in the range of 4 to 9 ps, the amplitude fluctuation and timing jitter of the recovered clock pulses

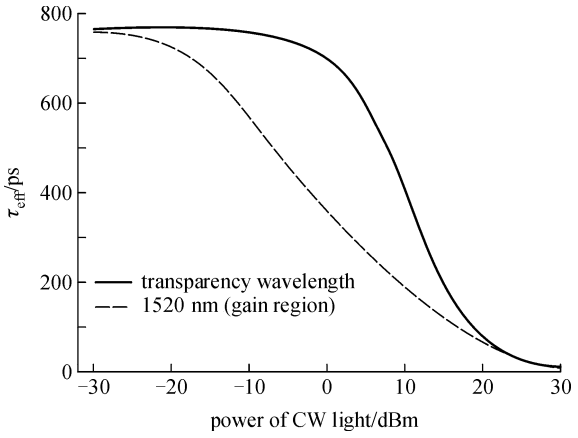

Fig. 3 τ_{eff} of SOA as a function of the power of assisting CW light

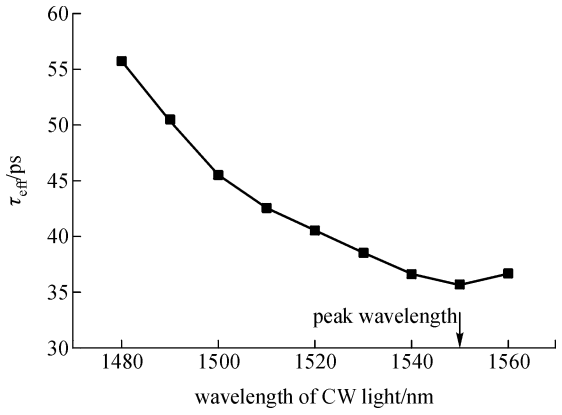

Fig. 4 τ_{eff} of SOA as a function of the wavelength of assisting CW light (input power is 25 dBm)

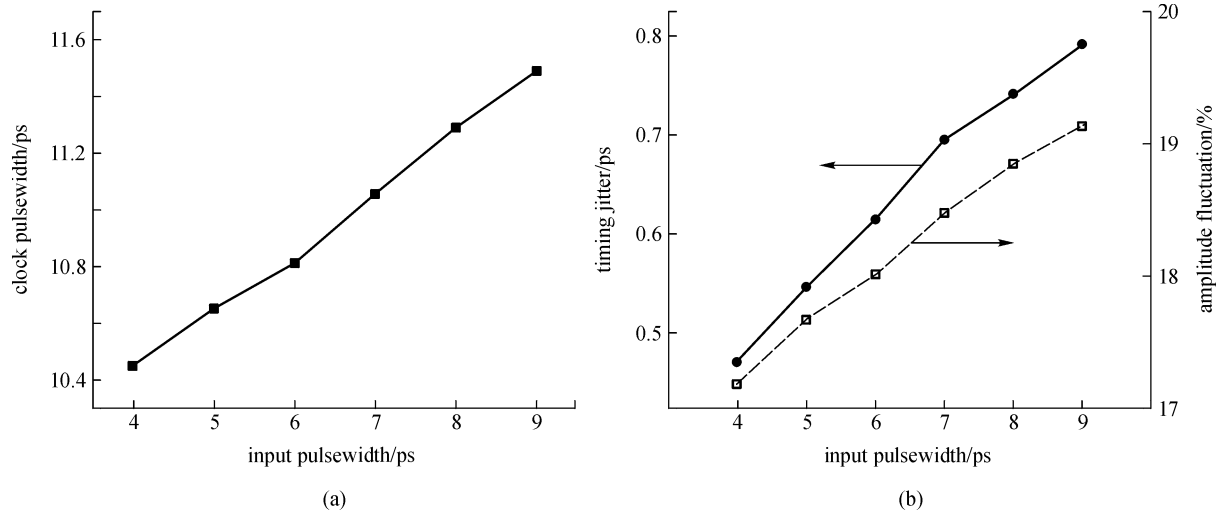

Fig. 5 Pulsewidth (a), amplitude fluctuation and timing jitter (b) of recovered clock pulses as a function of pulsewidth of injected CSRZ data (CW light power: 25 dBm, SOA bias current: 90 mA, average input power: 5.44 dBm)

are less than 20% and 1 ps, respectively, which show comparatively good performances.

The recovered clock pulsewidth, amplitude fluctuation and timing jitter versus the power of injected CSRZ data are plotted in Fig. 6. It is observed that with increasing data power, the recovered clock pulsewidth becomes narrower due to the stronger interaction of the clock and CSRZ data. Figure 6(b) shows that the average power of injected CSRZ data has an obvious effect on the quality of recovered clock pulses. The simulation results illustrated in Fig. 6(b) indicate that the recovered clock amplitude fluctuation and timing jitter increase against the power of the injected CSRZ data. Meanwhile, for CSRZ data power in the range of 3 to 8 mW, the amplitude fluctuation is reduced from 18% to 13.1% and timing jitter from 0.73 to 0.3 ps. Therefore, it is necessary to choose the appropriate injected light power.

Figure 7 shows the pulsewidth of recovered clock, amplitude fluctuation and timing jitter versus the injected SOA bias current. As seen from Fig. 7(a), the pulsewidth of clock signal increasingly becomes narrower as the bias current of SOA gradually increases. The principle is as follows: with increasing injected SOA bias current, the density of carriers will increase accordingly and lead to the reduction of the carrier lifetime. Thus, a shorter carrier lifetime will reduce the clock pulsewidth. Figure 7(b) indicates that with an increasing SOA bias current, the recovered clock amplitude fluctuation and timing jitter decrease accordingly to a certain extent. For injected SOA bias current in the range of 70 to 120 mA, the amplitude fluctuation is reduced from 17.5% to 15.4% and timing jitter from 0.9 to 0.3 ps.

Overall, appropriate power and pulsewidth of injected CSRZ data are important to the quality of the recovered

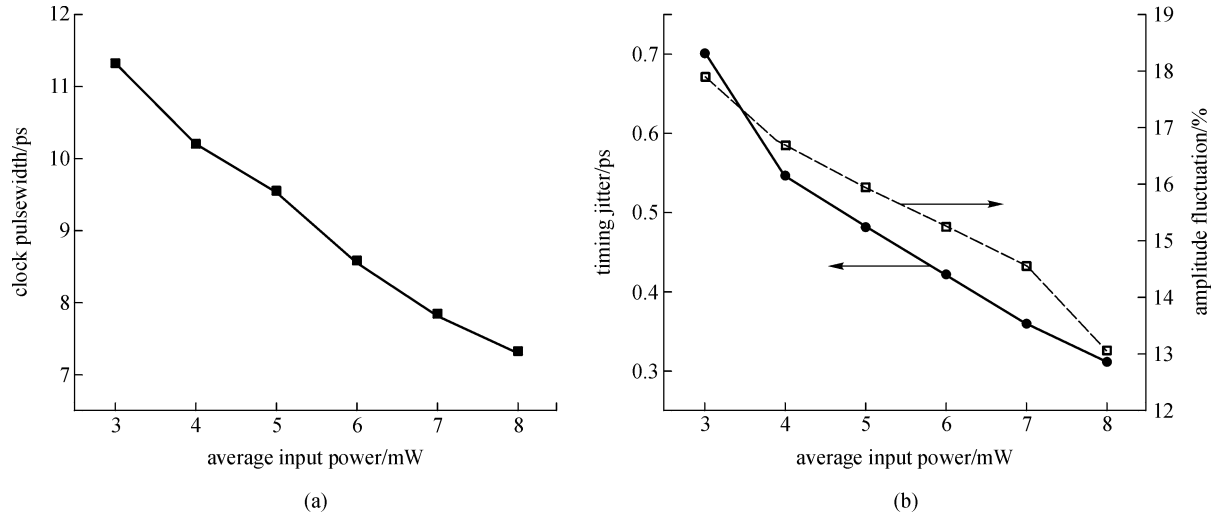

Fig. 6 Pulsewidth (a), amplitude fluctuation and timing jitter (b) of recovered clock pulses as a function of the average input power of injected CSRZ data (input pulsewidth: 5 ps, CW light power: 25 dBm, SOA bias current: 90 mA)

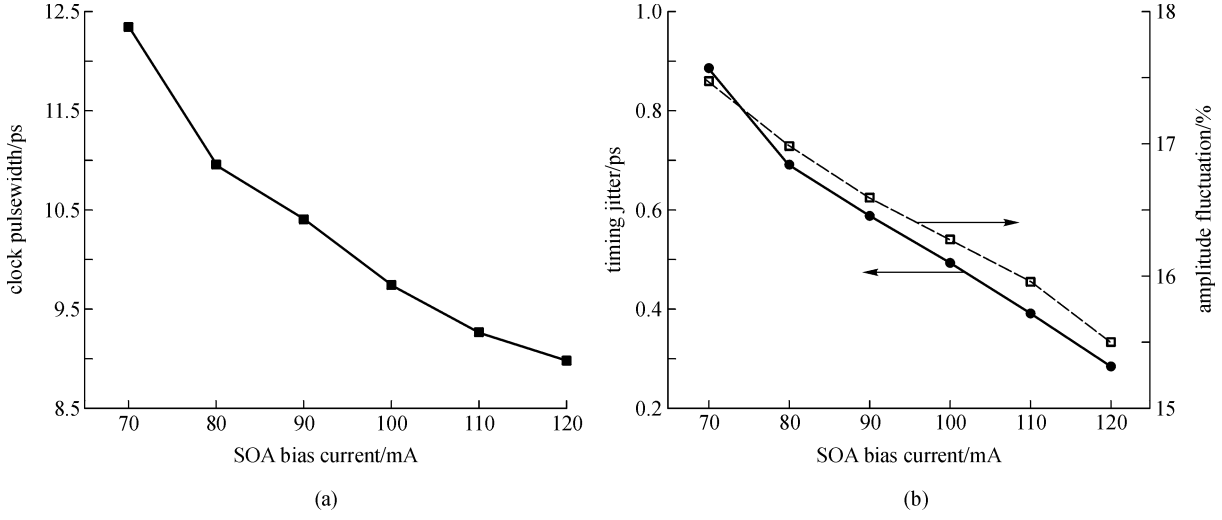

Fig. 7 Pulsewidth (a), amplitude fluctuation and timing jitter (b) of recovered clock pulses as a function of SOA bias current (input pulsewidth: 5 ps, CW light power: 25 dBm, average input power: 5.44 dBm)

clock in Figs. 5 and 6. Meanwhile, higher injected SOA bias current is necessary to the quality of the recovered clock in Fig. 7. To achieve ideal clock signals, analyzing important parameters is a useful guide to optimize this system.

4 Conclusion

In this paper, all-optical clock extraction from CSRZ modulation format data is investigated using an SOA-based ring laser for the first time. A model based on the laser is proposed for numerically analyzing the clock performance at a 40 Gbit/s rate. The results show that the pulsewidth, power of the injected CSRZ data and bias currents of SOA have a great influence on the performances of the recovered clock pulses such as amplitude fluctuation and timing jitter. Meanwhile, simulation results also show that high-quality clock extraction from 2^7–1 PRBS CSRZ data at 40 Gbit/s is realized by injecting higher assisting CW light into the SOA-based ring laser. It is believed that this simple scheme is an effective method for all-optical clock extraction and other all-optical signal processing.

Acknowledgements The authors would like to thank the Lin Jintong Lab, Key Laboratory of Optical Communication and Lightwave Technologies of Ministry of Education, Beijing University of Posts and Telecommunications for the support.

References

1. Brox O, Bauer S, Biletzke M, Ding H, Kreissl J, Wünsche H J, Sartorius B. Self-pulsating DFB for 40 GHz clock-recovery: impact of intensity fluctuations on jitter. In: Proceeding of Optical Fiber Communication Conference. 2004, paper MF55
2. Arahira S, Sasaki S, Tachibana K, Ogawa Y. All-optical 160-Gb/s clock extraction with a mode-locked laser diode module. IEEE Photonics Technology Letters, 2004, 16(6): 1558–1560
3. Kawanishi S, Saruwatari M. Ultra-high-speed PLL-type clock recovery circuit based on all-optical gain modulation in traveling-wave laser diode amplifier. Journal of Lightwave Technology, 1993, 11(12): 2123–2129
4. Patrick D M, Manning R J. 20 Gbit/s all-optical clock recovery using semiconductor nonlinearity. Electronics Letters, 1994, 30(2): 151–152
5. Lee D S, Lee M S, W Y J, Nirmalathas A. Electrically band-limited CSRZ signal with simple generation and large dispersion tolerance for 40-Gb/s WDM transmission systems. IEEE Photonics Technology Letters, 2003, 15(7): 987–989
6. Nezam S M R M, Luo T, McGeehan J E, Willner A E. Enhancing the monitoring range and sensitivity in CSRZ chromatic dispersion monitors using a dispersion-biased RF clock tone. IEEE Photonics Technology Letters, 2004, 16(5): 1391–1393
7. Chowdhury A, Raybon G, Essiambre R J, Doerr C R. WDM CSRZ 40 Gbit/s pseudo-linear transmission over 4800 km using optical phase conjugation. Electronics Letters, 2005, 41(3): 151–152
8. Greer E J, Smith K. All-optical FM mode-locking of fibre laser. Electronics Letters, 1992, 28(18): 1741–1743
9. Smith K, Lucek J K. All-optical clock recovery using a mode-locked laser. Electronics Letters, 1992, 28(19): 1814–1816
10. Wang Hui, Wu Jian, Lin Jintong. Spectral characteristics of optical pulse amplification in SOA under assist light injection. Journal of Lightwave Technology, 2005, 23(9): 2761–2771
11. Yin Lina, Liu Guoming, Wu Jian, Lin Jintong. Reduction of pattern effect for clock recovery based on semiconductor optical amplifier using CW assist light. Optical Engineering, 2006, 45(4): 045001
12. Hong Wei, Huang Dexiu, Sun Junqiang, Liu Deming. Numerical simulation of recovery enhancement by a CW pump light in semiconductor optical amplifiers. Optics Communications, 2002, 214(1–6): 335–341
13. Wang Tong, Lou Caiyun, Huo Li, Wang Zhaoxin, Gao Yizhi. Combination of comb-like filter and SOA for preprocessing to reduce the pattern effect in the clock recovery. IEEE Photonics Technology Letters, 2004, 16(2): 614–616